ULTRA HIGH PERFORMANCE FIBER REINFORCED CONCRETE UNDER CYCLIC LOADING

Spyridon A. Paschalis and Andreas P. Lampropoulos

Biography:

Spyridon A. Paschalis is a PhD candidate at the University of Brighton. He has graduated from the Department of Civil Engineering of the Democritus University of Thrace (2007). He holds an MSc in "Earthquake Engineering and Seismic Resistant Structures" from the Hellenic Open University (2013) and he has worked as a structural engineer in the private sector. His main research interest is focused on the Earthquake Strengthening of Structures.

Dr Andreas P. Lampropoulos is Senior Lecturer at the University of Brighton. He received his PhD from the University of Patras in 2010. His research agenda spans the areas of earthquake strengthening/retrofitting existing structures, new cement free concrete materials and Ultra High Performance Fiber Reinforced Concrete (UHPFRC). He has published more than 25 journal and conference papers and he serves as the Chair of IABSE Working Group 7 on 'Earthquake Resistant Structures'.

ABSTRACT

Ultra High Performance Fiber Reinforced Concrete (UHPFRC) is a novel cementitious material with enhanced strength in tension and compression and significantly high energy absorption in the post-cracking region. The application of UHPFRC for the earthquake strengthening of existing structures could considerably improve the performance of existing structures due to its superior properties. There are published studies where the direct tensile and the flexural behavior of UHPFRC have been investigated and the superior tensile

strength and post-crack energy absorption have been highlighted. However, there are not any published studies on the performance of UHPFRC under cyclic loading. In this paper, the results of an extensive experimental program on UHPFRC under direct tensile cyclic loading are presented and a constitutive model for the response of UHPFRC under cyclic loading is proposed. The accuracy of the proposed model is validated using experimental results from various loading histories and for different percentages of fibers, and the reliability of the proposed model is highlighted.

Keywords: UHPFRC; Cyclic Loading; Direct Tensile Tests; Constitutive model

INTRODUCTION

Ultra High Performance Fiber Reinforced Concrete (UHPFRC) is a relative new material with high strength and durability. Some of the main characteristics of UHPFRC are the high compressive strength (normally in the range of 150-200 MPa (21.8-29 ksi)), the high tensile strength which can reach values more than 15 MPa (2.2 ksi), the ductile behavior, and finally the durability and the significantly high energy absorption in the post cracking region.

There are published studies where the behavior of UHPFRC under static loading has been investigated (Kang et al.[1], Kang & Kim[2], Hassan et al.[3], Yoo et al.[4], Nguyen et al.[5]). The effect of the steels fibers amount was examined by Kang et al.[1] (2010) and Yoo et al.[4] (2013) and it was found that the flexural strength was considerably increased as the fiber volume ratio was increased, while the ductility was decreased. Inverse analysis (Kang et al.[1]) was used to determine the direct tensile fracture model of UHPFRC, and a tri-linear tensile fracture model of UHPFRC with a softening branch was proposed. Another important parameter in case of UHPFRC is the orientation and the distribution of steel fibers in the mix.

This parameter can considerably affect the post-cracking behavior but the effect on the pre-cracking elastic phase is negligible (Kang & Kim[2]).

All these studies are focused on the mechanical properties of UHPFRC under static loading. However, there are not any available studies on the behavior of UHPFRC under cyclic loading, even if the behavior of the material under cyclic loading is of high importance in earthquake prone areas. The main aim of this study is to investigate the behavior of UHPFRC under cyclic loading and to develop a constitutive model for the tensile stress-strain characteristics of the material under cyclic loading. The proposed model is based on previously published models on the cyclic behavior of conventional concrete. Yankelevsky and Reinhardt[6] proposed a stress-strain model for normal concrete under cyclic tension. In this model, using seven geometrical points, the unloading and reloading curves were constructed as linear parts. Yankelevsky and Reinhardt[7] developed a model for concrete subjected to cyclic compression. In this model the same principles as the model of Yankelevsky and Reinhardt[6] for concrete under tension were used. This model was based on the envelope curve which was assumed to be independent of the loading history, and the unloading –reloading curves were composed by linear parts using six focal points. Sima et al.[8] presented a model for the cyclic response of concrete in both tension and compression. The modulus of elasticity and the strength degradation with the cycles were both taken into account, and the reliability of the model under various cyclic loading histories was highlighted. Aslani and Jowkarmeimandi[9] developed a constitutive model for unconfined concrete subjected to cyclic tension and compression. In this model, the unloading curves were considered non-linear, while the reloading curves were considered linear and the degradation of the modulus of elasticity was taken into consideration.

Mander et al.[10] proposed a stress-strain relation for reversed loading. For this model, the envelope curve was considered identical to the monotonic stress-strain curve. For the

simulation of the monotonic curve a modified equation proposed by Popovic[11] was used. The unloading and reloading branches of the model were calibrated using available experimental results. Martinez-Rueda and Elnashai[12] proposed a modified model based on the model proposed by Mander et al.[10], which takes into consideration strength and modulus of elasticity degradation under increased strain values.

In the present study, the results of an extensive experimental program on UHPFRC under direct tensile loading are presented first. Various loading histories and different percentages of steel fibers have been investigated and the stress-axial strain responses have been recorded. These experimental results have been used for the development of a constitutive stress-axial strain model of UHPFRC under cyclic loading. The accuracy of the proposed model is validated using experimental results with various loading histories and for different percentages of steel fibers, while the reliability of the proposed model is highlighted.

RESEARCH SIGNIFICANCE

The use of UHPFRC for earthquake resistant structures is a novel application. In earthquake prone areas the structures, and subsequently the load bearing elements, are subjected to seismic loads which are usually simulated with a cyclic loading history. The cyclic response of the structural elements is highly affected by the behavior of the materials under cyclic loading. However, there are not any previously published studies on UHPFRC under cyclic loading. The current study aims to address this research gap by presenting the results of an extensive experimental investigation. These results have been used for the constitutive modeling of the behavior of UHPFRC under cyclic loading. The proposed model can accurately predict the response of UHPFRC under various loading histories and for different percentages of steel fibers while the reliability of the model is evidenced by comparisons with experimental data.

EXPERIMENTAL INVESTIGATION

In the current experimental investigation, direct tensile tests of UHPFRC under monotonic and cyclic loading were conducted. Different percentages of steel fibers were examined in order to investigate the effect of the amount of steel fibers on the tensile strength of UHPFRC. Cyclic loading tests under various loading histories were performed and a model for the response of UHPFRC under cyclic loading was proposed. The proposed model was validated for the different loading histories and the different percentages of steel fibers. Detailed description of the material preparation procedure and the experimental setup are presented in the following sections.

Mix design and specimens' preparation

One of the main characteristics of UHPFRC is the enhanced homogeneity which is achieved by the use of fine aggregates only. Hence, in the mix silica sand with maximum particle size of 500 μm (0.01969 in) and compacted bulk density of 1587 kg/m^3 (98.4 lb/ft^3) was used together with dry silica fume with bulk density 200-350 kg/m^3 (12.4-21.7 lb/ft^3) and retention on 45 μm (0.00177 in) sieve < 1.5 %, Ground Granulated Blast Furnace Slag (GGBS) with density 2400-3000 kg/m^3 (148.8-186 lb/ft^3) and cement I class 32.5 N. Micro silica with fine particles was used in order not only to increase the density of the matrix but also to improve the rheological properties of the mix. Low water/cement ratio was also used together with polycarboxylate superplasticizer. In the examined mix, 3 different percentages of steel fibers, 1%, 2% and 3% per volume were used. The steel fibers had length 13 mm (0.51181 in), diameter 0.16mm (0.0063 in) , tensile strength 3000 MPa (435 ksi) while the modulus of elasticity had value 200 GPa (29 Msi). The examined mix (Table 1) was based on a previous study (Hassan et al.[3] 2012)

Regarding the mixing procedure, all the dry ingredients were mixed initially for 3 minutes. Then, water and superplasticizer were added to the mix and once the mix was wet, steel fibers were added gradually. A high shear mixer (Zyklos Pan Mixer ZZ 75 HE) was used for the mixing of the materials. After the demoulding, the specimens were placed in a water curing tank for 28 days. The specimens were tested 3 months after the casting.

Experimental setup

Dog-bone specimens were used for the direct tensile tests. In total, 25 identical dog bone specimens were examined using different percentages of steel fibers and different loading histories. A rectangular cross section at the neck 13mm*50mm (0.512in*1.969in) was used. The geometry of the examined specimens is illustrated in Figure 1. The tests were conducted using Instron 8500 testing machine. The extension was recorded using a Linear Variable Differential Transformer (LVDT) connected to a special steel frame (Figure 2b). This setup was used in order to measure directly the average of the extensions on both sides of the specimens. A number of specimens were also monitored using LaVision Digital Image Correlation System (Figure 2a) and the extension was found to be in perfect agreement with the LVDT measurements. The tests were controlled by the LVDT measurements, using a constant displacement rate of 0.007 mm/sec (0.00028 in/sec). Three different loading histories were used in this investigation (Figure 3). Extension step of 0.2 mm (0.00789 in) was used for loading history 1, while for loading histories 2 and 3 the step was equal to 0.4 mm (0.01578 in) and 0.8 mm (0.02367 in) respectively (Figure 3).

Experimental results and discussion

Initially, the performance of UHPFRC under monotonic loading was investigated. For this reason, 6 monotonic tests of dog bone specimens with 3% steel fibers were conducted and the

stress- axial strain curves together with the average curve are presented in Figure 4. The respective stress-axial strain results for the specimens tested under cyclic loading for the loading histories 1, 2 and 3 are presented in Figures 5a, 5b and 5c respectively. Additionally, in table 2, average stress and axial strain values for characteristic points at the end of the linear part and at the maximum stress are presented. These results (table 2) indicate that there is a significant strain hardening branch from the end of the linear part of the stress-axial strain curve until the ultimate stress value.

The experimental results of Figure 5 were used for the calculation of the modulus of elasticity degradation with the number of cycles. The results for all the identical specimens together with the average distributions and the bilinear approximations, for loading histories 1, 2 and 3 are presented in Figures 6a, 6b and 6c respectively.

From Figure 6 it is evident that the modulus of elasticity was considerably reduced after the first loading cycle in all the examined loading cases and then it was slightly further reduced as the number of cycles was increased. In all the examined cases the modulus of elasticity was approximately reduced to the 25% of its initial value after the first loading cycle. This significant reduction is mainly attributed to the fact that in all the examined loading histories, the response of the specimens reached the post-cracking phase at the first loading cycle (Figure 5).

The average curve of all the examined cases is presented in Figure 7. Based on these results (Figure 7), equation 1 is proposed for the reduction of the modulus of elasticity with the loading cycles. This equation was also used for the bilinear approximations of figure 6 and it can be observed that the results obtained using equation 1 are in very good agreement with the experimental results.

$$\frac{E_n}{E_0} = (0.25 - 0.016 \cdot n) \quad (1)$$

where:

n: is the number of cycles, n>1

E_0: is the initial modulus of elasticity,

E_n: is the modulus of elasticity after n cycles.

The comparison between the average experimental results and the proposed model is presented in Figure 8. The results of the bilinear models indicate that the behavior is not affected by the loading history and is governed by the same equation 1 in all the examined cases.

ANALYTICAL INVESTIGATION

The response of UHPFRC in direct tension is dissimilar to the response of conventional plain concrete under the same loading condition. The behavior of concrete in tension is considered linear up to the maximum level of stress and after this point a sudden failure occurs. On the contrary, for UHPFRC after the linear part in which the steel fibers don't have any effect, the first crack appears and we have a non-linear behavior up to the maximum load. After this point the stress drops gradually. These phases of UHPFRC under tension can be distinguished in figure 9.

In the present study, the envelope curve for cyclic loading is assumed identical to the monotonic stress-axial strain response. This assumption has also been adopted by other researchers (Yankelevsky and Reinhardt[6] and Bahn and C. T. Hsu[13]). In figure 10 the average monotonic curve is presented together with the respective results of cyclic loading tests. The results indicate that the average monotonic curve is approaching the cyclic response of the specimens.

The proposed model is consisted of 5 various phases as presented in figure 9. The first is the linear phase up to a level of stress f_0 and axial strain ε_0. The second is the non-linear phase up to a maximum stress of f_c and axial strain ε_c. The third is the descending phase until the unloading point (f_{un}, ε_{un}), and finally the next 2 phases are the unloading and the reloading phases. In the first part, the stress-strain relation is linear, hence it is given from the equation 2.

$$\sigma=\varepsilon \cdot E_0 \quad \text{for } \varepsilon \leq \varepsilon_0 \tag{2}$$

where:

ε: is the axial strain,

E_0 : is the modulus of elasticity,

After the elastic part, the behavior of the material is characterized by an ascending non-linear branch until the maximum stress. This is the phase where the cracking of the concrete matrix occurs and the steel fibers are bridging the micro-cracks. After this point, the stress falls gradually due to the localization of the damage. This non-linear behavior is described by an exponential curve. Hence, two equations are proposed for both the ascending part (from the elastic limit until the maximum stress limit), as well as the descending branch from the maximum stress limit up to the unloading point. Therefore, for the ascending part the following equation 3 is proposed:

$$\sigma=\varepsilon_0 \cdot (1-A)+A \cdot \varepsilon \cdot e^{\frac{(\varepsilon_0-\varepsilon)}{\varepsilon_c}} \tag{3}$$

where:

ε_0: is the axial strain at the end of the linear part,

ε_c: is the respective axial strain for the maximum stress,

A is given from the equation (4).

$$A=\frac{f_c-\varepsilon_0\cdot E_0}{E_0\cdot(\varepsilon_c\cdot e^{(\frac{\varepsilon_0}{\varepsilon_c}-1)}-\varepsilon_0)} \quad (4)$$

where f_c is the maximum stress

These equations were initially proposed by Mazars and G. Pijaudier-Cabot[14] and they were also used by other researchers (Sima et al.[8], Faria et al.[15], Saetta et al.[16]).

For the descending branch and taking into consideration the softening part, Sima et al.[8] considered an exponential curve and took into consideration a point on the envelope curve. This exponential curve is also adopted for UHPFRC in the descending branch. Therefore, the descending curve is described by the equation 5:

$$\sigma=(B+C\cdot\varepsilon\cdot e^{(\frac{\varepsilon_0-\varepsilon)}{\varepsilon_c}})\cdot E_0 \text{ for } \varepsilon>\varepsilon c \quad (5)$$

where:

$$B=\frac{f_{op}\cdot\varepsilon_c\cdot e^{(\frac{\varepsilon_0}{\varepsilon_c}-1)}-\varepsilon_{op}\cdot f_c\cdot e^{\frac{\varepsilon_0}{\varepsilon_c}\cdot(1-\frac{\varepsilon_{op}}{\varepsilon_0})}}{E_0\cdot(\varepsilon_c\cdot e^{(\frac{\varepsilon_0}{\varepsilon_c}-1)}-\varepsilon_{op}\cdot e^{\frac{\varepsilon_0}{\varepsilon_c}\cdot(1-\frac{\varepsilon_{op}}{\varepsilon_0})})} \quad (6)$$

$$C=\frac{f_c-f_{op}}{E_0\cdot(\varepsilon_c\cdot e^{(\frac{\varepsilon_0}{\varepsilon_c}-1)}-\varepsilon_{op}\cdot e^{\frac{\varepsilon_0}{\varepsilon_c}\cdot(1-\frac{\varepsilon_{op}}{\varepsilon_0})})} \quad (7)$$

where:

ε_{op}: is the axial strain at any point on the descending part of the stress-axial strain curve,

f_{op}: is the respective stress at any point on the descending part of the stress-axial strain curve.

Previous studies on plain concrete (Sinha et al.[17]) indicate that during the unloading phase, the modulus of elasticity is high at the beginning, then gradually drops, and finally becomes flat. Based on the experimental results of the present study, the unloading branch of UHPFRC exhibits a different behavior which is attributed to the presence of steel fibers in the mix. For this reason, the experimental results have been used for the calibration of the constitutive model. The equation proposed by Sima et al.[8] for the unloading part has been calibrated in order to fit the experimental results (equation 8). From the validation of the proposed model and using all the experimental results of the various mixes it was evident that this equation can accurately predict the behavior of UHPFRC in this branch.

$$\sigma = D \cdot e^{\frac{F \cdot \left(1-\frac{\varepsilon-\varepsilon_{pl}}{\varepsilon_{un}-\varepsilon_{pl}}\right)}{22}} \cdot E_0 \cdot (\varepsilon-\varepsilon_{pl}) \quad (8)$$

where :

$$D = \frac{r \cdot (1-\delta_{un})}{r-1} \quad (9)$$

$$r = \frac{\varepsilon_{un}}{\varepsilon_{pl}} \quad (10)$$

ε_{pl}: is the residual axial strain for the unloading curve for zero stress,

ε_{un}: is the unloading axial strain,

δun: is the compressive damage at the unloading point and is given from equation (11).

$$\delta_{un} = 1 - \frac{B}{\varepsilon} - C \cdot e^{\left(\frac{\varepsilon_0 - \varepsilon}{\varepsilon_c}\right)} \quad (11)$$

F is given from the equation (12).

$$F = \mathrm{Ln}\left(\frac{R \cdot (1-\delta_{un}) \cdot (r-1)}{r}\right) \quad (12)$$

R is given from the equation (13)

$$R = \frac{E_{pl}}{E_0} \quad (13)$$

where E_{pl} is the Modulus of elasticity at the end of the unloading curve.

The experimental results presented in this study indicate that the modeling of the re-loading part with a linear stress-strain equation, which is adopted for conventional concrete, can't accurately predict the response of UHPFRC. Hence, an exponential equation, which is a modification of equation 3, is proposed in order to describe the behavior of the reloading curves of UHPFRC (Equation 14).

$$\sigma = \left(\varepsilon_{0'} \cdot (1-A') + A' \cdot \varepsilon \cdot e^{\left(\frac{\varepsilon_{0'} - \varepsilon}{\varepsilon_{c'}}\right)}\right) \cdot E_{0'} \quad (14)$$

where:

A: is given from the equation (15)

$$A'=\frac{f_{c'}-\varepsilon_{0'}\cdot E_{0'}}{E_{0'}\cdot(\varepsilon_{c'}\cdot e^{(\frac{\varepsilon_{0'}}{\varepsilon_{c'}}-1)}-\varepsilon_{0'})} \quad (15)$$

$f_{c'}$: is the maximum stress at the reloading curve,

$\varepsilon_{c'}$: is the axial strain for the respective maximum stress in the descending curve,

$\varepsilon_{c'}=\varepsilon-\varepsilon_{pl,}$

$E_{0'}$: is the initial tangent modulus of elasticity,

$\varepsilon_{0'}$: is the respective maximum strain for the tangent modulus of elasticity.

VALIDATION OF THE PROPOSED CONSTITUTIVE MODEL

Experimental results of all the examined loading histories for specimens with 3% steel fibers were used for the validation of the model. In figures 11a, 11b and 11c the results of the proposed constitutive model are compared with experimental results for loading histories 1, 2 and 3 respectively. From these figures it is evident that the results of the proposed model are in very good agreement with the respective experimental results. Therefore, it can be concluded that the proposed model can accurately predict the cyclic response of UHPFRC.

The required parameters of the proposed model (i.e. the modulus of elasticity and the stress and axial strain at the end of the elastic part and at the maximum stress level) can be calculated from the monotonic stress-axial strain results. For the degradation of the modulus of elasticity with the loading cycles, the proposed model of equation 1 can be adopted, which was validated in the previous section (figure 8).

INVESTIGATION OF THE EFFECT OF DIFFERENT PERCENTAGES OF STEEL FIBERS

Effect of steel fibers on the tensile strength of UHPFRC

An additional investigation was conducted on the effect of steel fibers volume on the behavior of UHPFRC. Specimens with percentages 1% and 2% were tested under monotonic loading additionally to the specimens with 3% steel fibers (Table 1). Higher percentages of steel fibers were not investigated since the use of higher steel fiber volumes is not a cost effective way to achieve superior mechanical properties. This was also highlighted by Ferrara et al.[18]. According to this study (Ferrara et al.[18]), high mechanical properties can be achieved even with low percentage of fibers (around 1%) by controlling steel fiber orientation.

The experimental results for all the examined mixes together with the average monotonic curves are presented in figures 12 and 13. Also, the average values for the stress and axial strain at the end of the elastic part and at the maximum stress level for the specimens with steel fibers volume 1% and 2% are presented in tables 3 and 4 respectively.

From tables 2, 3 and 4, it is evident that the elastic part is not affected by the volume of steel fibers in the mix. Also, it is obvious that as the steel fiber percentage is increased, the maximum stress value is improved and the strain hardening phase is increased. The same observation can be made from the results presented in figure 14. In this figure, the increment of the tensile strength with the steel fibers volume is presented. The experimental results indicate that when steel fibers volume was increased from 1% to 2%, tensile strength increment of 23.1% was observed. Further increment of steel fibers volume from 2% to 3% resulted in 4.3% increment of the maximum tensile strength.

UHPFRC under cyclic loading for different percentages of steel fibers

The results of the previous section indicated that strain hardening behavior can be achieved with a minimum percentage of steel fibers 2%. Hence, in order to investigate the reliability of the proposed model for percentages other than 3%, cyclic loading tests (loading history 2, figure 3) were conducted for specimens with 2% steel fibers.

The experimental results are presented in figure 15 and the validation of the proposed model is presented in figure 16. From figure 16 it is evident that the proposed model can accurately predict the response of UHPFRC for percentage of steel fibers 2%.

CONCLUSIONS

In the present study, the response of various UHPFRC mixes under tensile monotonic and cyclic loading was investigated.

Monotonic tests were conducted on specimens with 1%, 2% and 3% steel fibers volume, and the experimental results indicated that when steel fibers volume was increased from 1% to 2%, tensile strength increment of 23.1% was observed. Further increment of steel fibers volume from 2% to 3% resulted to 4.3% increment of the maximum tensile strength. From this investigation it was evident that the elastic part was not affected by the volume of steel fibers, while the strain hardening phase was increased. Based on these results, strain hardening behavior was achieved using 2% minimum percentage of steel fibers. This was the minimum percentage which was used in the current study for specimens tested under cyclic loading.

Specimens with 2% and 3% of steel fibers were tested under cyclic loading and a constitutive model for the tensile stress versus axial strain under cyclic loading was proposed. The accuracy of the model was validated using experimental results of specimens with various percentages of steel fibers tested under different loading histories, and the reliability of the proposed model was highlighted. The experimental results of the present study were also used for the calculation of the modulus of elasticity degradation with the number of loading cycles. The results indicated that the modulus of elasticity was considerably reduced after the first loading cycle in all the examined loading cases, and then it was slightly further reduced as the number of loading cycles was increased. Based on these results, a model for the reduction of the modulus of elasticity with the loading cycles was proposed.

ACKNOWLEDGMENTS

The authors would like to express their gratitude to Dr David Pope for his assistance during the testing, and they would also like to acknowledge Hanson Heidelberg Cement Group and Sika Limited for providing raw materials. The authors would also like to thank the anonymous reviewers for their valuable comments and suggestions which have considerably improved the manuscript.

NOTATION:

ε :The axial strain in the linear part.

E_0 : The modulus of elasticity.

ε_0 :The axial strain at the end of the linear part.

ε_c :The respective axial strain for the maximum stress.

fc :The maximum stress.

ε_{op} : The axial strain at any point on the descending part of the stress-strain curve.

f_{op} : The stress at any point on the descending part of the stress-strain curve.

ε_{pl} :The residual axial strain for the unloading curve for no stress.

ε_{un} :The unloading axial strain.

δ_{un} : The damage at the unloading point.

E_{pl} :The modulus of elasticity at the end of the unloading curve.

$f_{c'}$:The maximum stress at the reloading curve.

$\varepsilon_{c'}$:The axial strain for the respective maximum stress in the descending curve and $\varepsilon_{c'}=\varepsilon-\varepsilon_{pl}$

$E_{0'}$:The initial tangent modulus of elasticity at the beginning of the reloading curve.

$\varepsilon_{0'}$:The respective maximum axial strain for the tangent modulus of elasticity.

REFERENCES

1. Kang, S.T., Lee, Y., Park Y.D. and Kim, J.K., "Tensile fracture properties of an Ultra High Performance Fiber Reinforced Concrete (UHPFRC) with steel fiber." Composite Structures, V.92 , No 1, 2010, pp 61-71.

2. Kang, S.T. and Kim, J.K. "The relation between fiber orientation and tensile behavior in an Ultra High Performance Fiber Reinforced Cementitious Composites (UHPFRCC)." Cement and Concrete Research, V. 41, No.10, 2011, pp. 1001-1014.

3. Hassan, A.M.T., Jones, S.W. and Mahmud, G.H. "Experimental test methods to determine the uniaxial tensile and compressive behavior of Ultra High Performance Fiber Reinforced Concrete (UHPFRC)." Construction and Building Materials, V.37, 2012, pp.874-882.

4. Yoo, D.Y., Park, J.J, Kim, S.W. and Yoon, Y.S., "Early age setting, shrinkage and tensile characteristics of ultra high performance fiber reinforced concrete." Construction and Building Materials, V.41, 2013, pp. 427-438.

5. Nguyen, D.L., Kim, J.K, Ryu, G.S. and Koh, K.T., "Size effect on flexural behavior of ultra-high-performance hybrid fiber-reinforced concrete." Composites Part B: Engineering, V.45, No.1, 2013, pp.1104-1116.

6. Yankelevsky, D. Z. and Reinhardt, H.W., "Uniaxial Behavior of Concrete in Cyclic Tension." Journal of Structural Engineering, V.115, No1.,1989.

7. Yankelevsky, D.Z. and Reinhardt, H.W., "Model for Cyclic Compressive Behavior of Concrete." Journal of Structural Engineering V. 113, No.2, 1987.

8. Sima, J.F., Roca, P. and Molins, C,. "Cyclic Constitutive Model for Concrete." Engineering Structures, V.30, No.3, 2008, pp. 695-706.

9. Aslani, F. and Jowkarmeimandi, R., "Stress-strain model for concrete under cyclic loading." Magazine of Concrete Research, V.64, No.8, 2012, pp. 673-685.

10. Mander, J.B., Priestley, M.J and Park, R. "Theoretical Stress-Strain Model for Confined Concrete." Journal of Structural Engineering, V.114, No.8.,1988.

11. Popovics, S., (1973)"A numerical approach to the complete stress-strain curves for concrete",Cement and Concr. Res.,Vol.3, No.5, 1973, pp.583-599.

12. Martinez-Rueda, J.E. and Elnashai, A.S., "Confined Concrete model under cyclic load " Material and Structures, V.30, 1997, pp. 139-147.

13. Bahn, B. Y. and Hsu, C.T "Stress-strain behavior of concrete under cyclic loading." ACI Materials Journal, V.95, No.2, 1998,pp.178-193.

14. Mazars, J. and Pijaudier-Cabot, G. (1989). "Continuum damage theory. Application to concrete." Journal of Engineering Mechanics, V.115, No.2, 1998, pp. 345-365.

15. Faria, R., Oliver, J. and Cervera, M., "A strain based plastic viscous -damage model for massive concrete structures." International Journal of Solids and Structures , V.34 No.14, 1999, pp. 1533-1558.

16. Saetta, A., Scotta, R. and Vitaliani, R., "Coupled Environmental -Mechanical damage model of RC structures." Journal of Engineering Mechanics , V.128, No.8, 1999, pp. 930-940.

17. Sinha, B.P., Gerstle, K.H. and Tulin, L.G. "Stress-Strain Relations for Concrete Under Cyclic Loading." Journal of American Concrete Institute V.61, No.2., 1964.

18. Ferrara, L. , Ozyurt, N., Di Prisco, M., “High mechanical performance of fibre reinforced cementitious composites: the role of "casting-flow induced" fibre orientation.” Material and Structures 2011, V.44, No1, pp. 109-128.

TABLES AND FIGURES

List of Tables:

List of Figures:

Figure 11- Validation of the proposed model using experimental results for 3 different loading histories and 3% steel fibers

Figure 12- Monotonic stress-axial strain curves for specimens with 1% steel fibers

Figure 13- Monotonic stress-axial strain curves for specimens with 2% steel fibers

Figure 14- Tensile strength for different percentages of steel fibers

Figure 15- Stress-axial strain curves of UHPFRC with 2% steel fibers under cyclic loading

Figure 16- Validation of the proposed model for percentage of steel fibers 2%

Table 1 – UHPFRC mix design for specimens with different percentages of steel fibers

Material	Mix proportions (kg/m^3)		
Cement	657		
GGBS	418		
Silica fume	119		
Silica Sand	1051		
Superplasticizers	59		
Water	185		
Steel fibers (13mm length (0.5118 in) and 0.16 mm (0.0063 in) diameter)	235.5 (3% Steel fibers)	157 (2% steel Fibers)	78.5 (1% steel fibers)

Note: 1 kg/m^3=0.062 lb/ft^3 and 1mm=0.03937 in

Table 2 –Average stress and axial strain values for specimens with 3% steel fibers

Stress Level	Stress (MPa)	Axial Strain
End of Elastic	6.3	0.00013
Maximum Stress	8.9	0.01

Note: 1MPa= 0.145 ksi

Table 3–Average stress and axial strain values for specimens with 1% steel fibers

Stress Level	Stress (MPa)	Axial Strain
End of Elastic	6.0	0.00014
Maximum Stress	6.6	0.0008

Note: 1MPa= 0.145 ksi

Table 4–Average stress and axial strain values for specimens with 2% steel fibers

Stress Level	Stress (MPa)	Axial Strain
End of Elastic	7.0	0.00015
Maximum Stress	8.1	0.00094

Note: 1MPa= 0.145 ksi

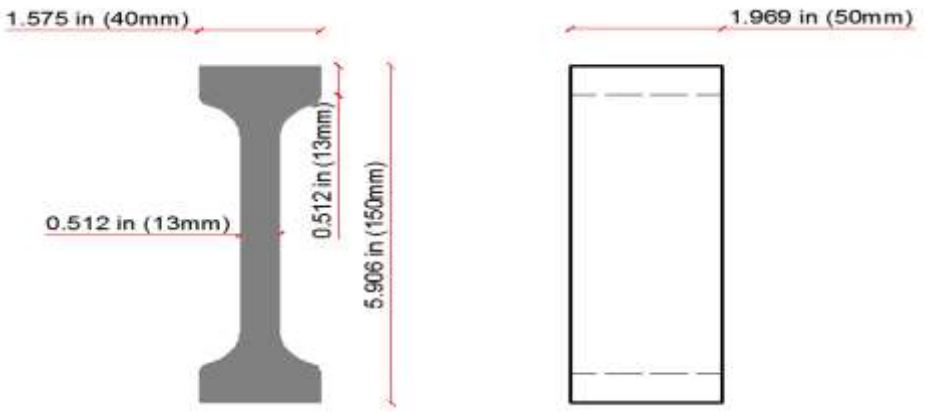

(Note: 1 mm=0.03937 in)

Figure 1 - Dog bone specimen

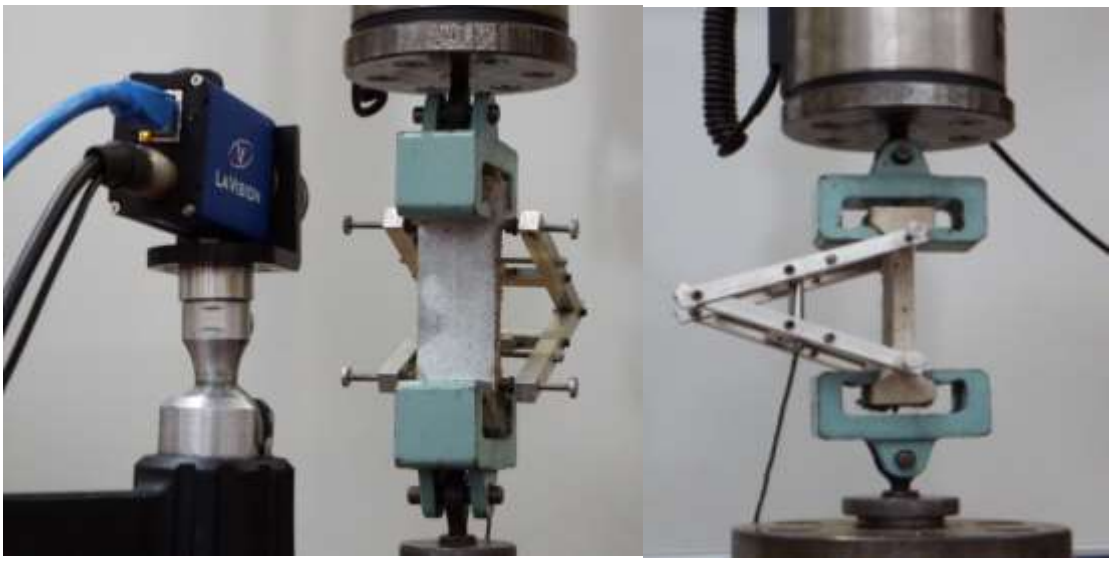

(a) **(b)**

Figure 2-Experimental setup

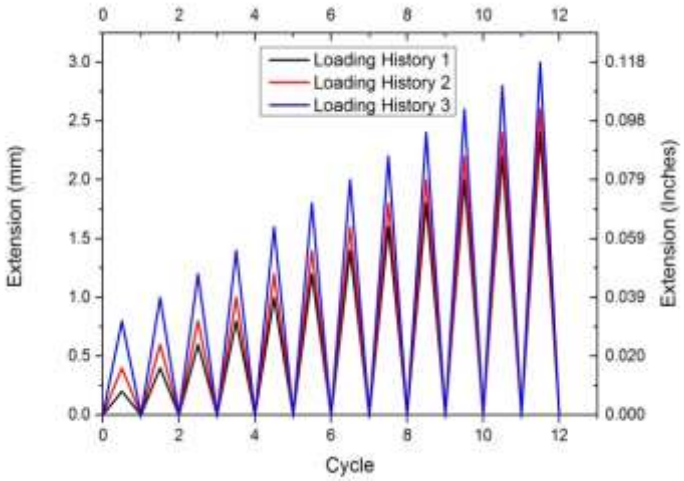

(Note: 1 mm=0.03937 in)

Figure 3- Examined loading histories

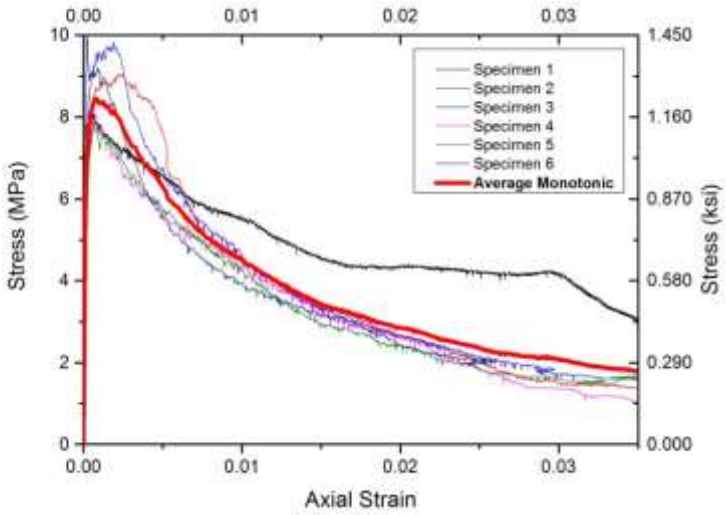

(Note: 1MPa= 0.145 ksi)

Figure 4- Monotonic stress-axial strain curves for specimens with 3% steel fibers

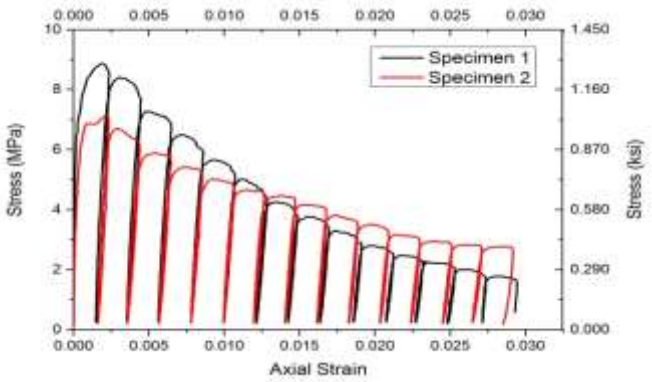

(a)

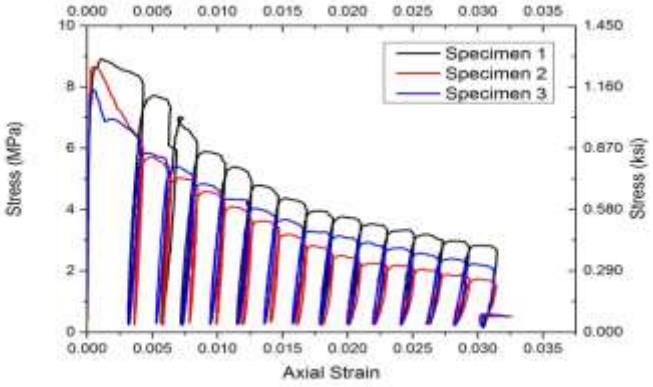

(b)

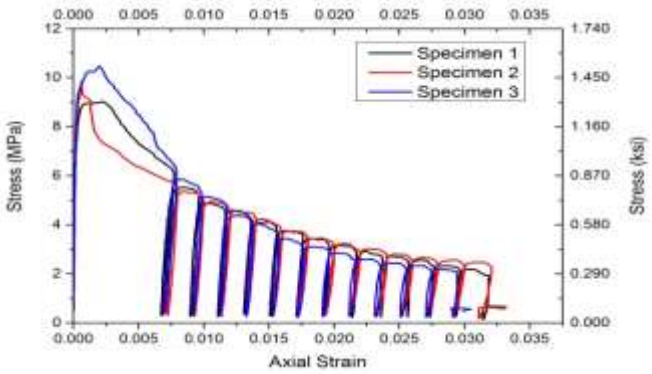

(c)

(Note: 1MPa= 0.145 ksi)

Figure 5– Experimental results for a) loading history 1, b) loading history 2, and c) loading history 3

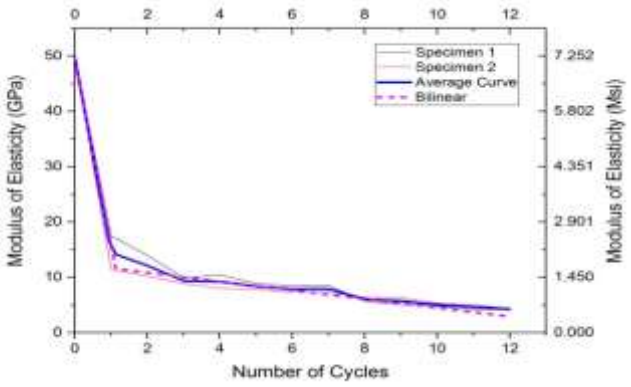

(a)

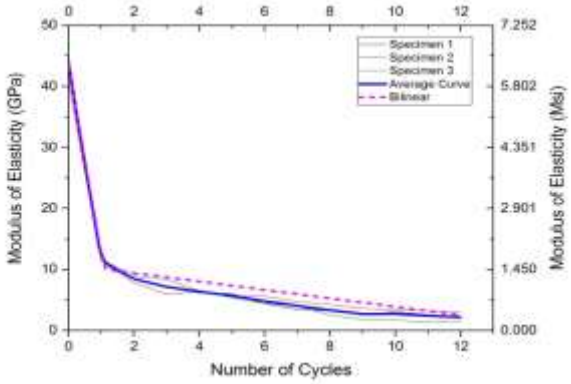

(b)

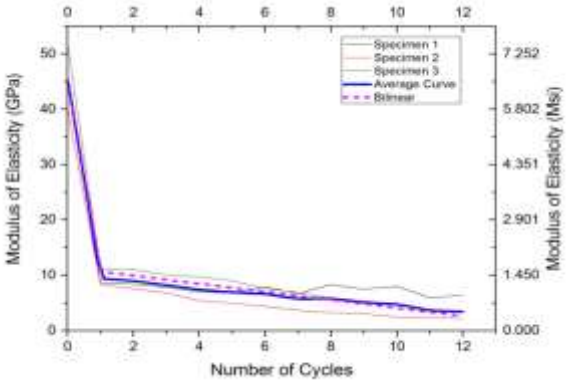

(c)

(Note: 1 GPa=0.145 Msi)

Figure 6– Modulus of elasticity degradation for a) loading history 1 b) loading history 2 c) loading history 3

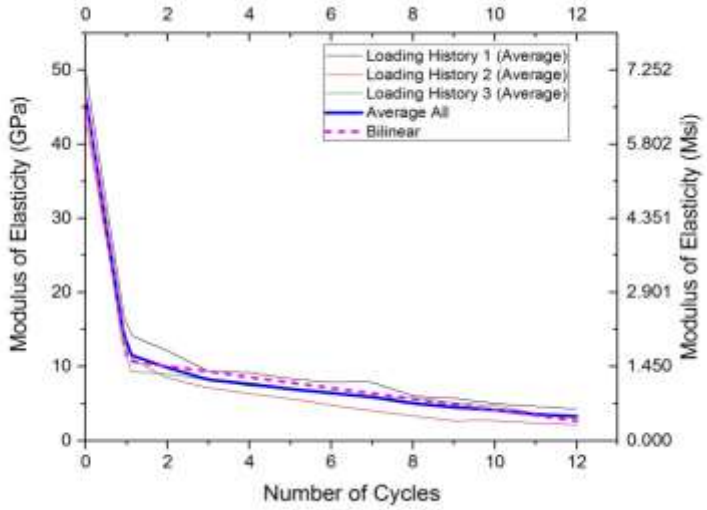

(Note: 1 GPa=0.145 Msi)

Figure 7- Average curves of the modulus of elasticity degradation for all the loading histories

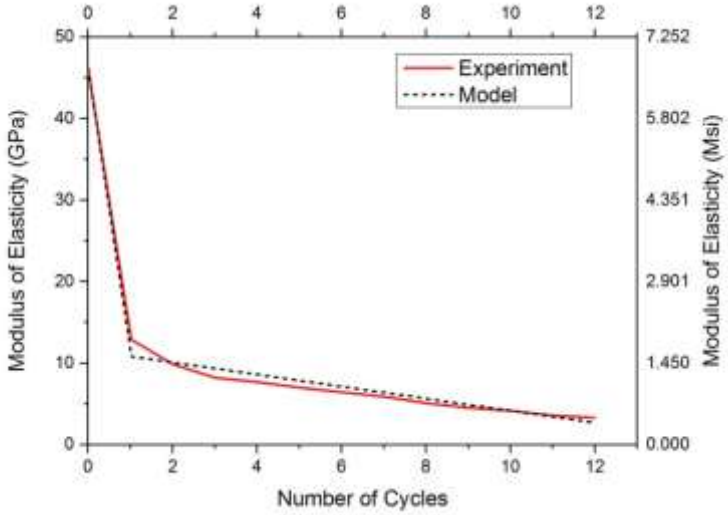

(Note: 1 GPa=0.145 Msi)

Figure 8- Degradation of the modulus of elasticity with the loading cycles

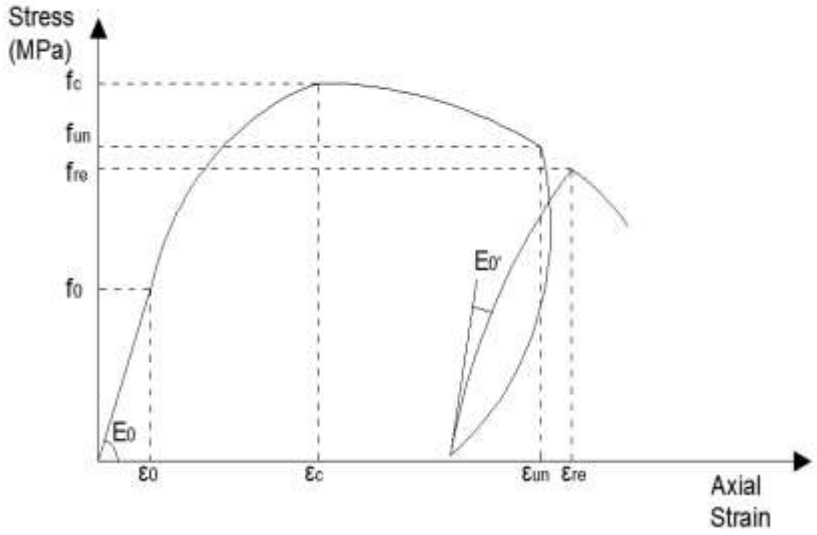

Figure 9- Stress-Axial Strain Curve of UHPFRC under cyclic loading

(Note: 1MPa= 0.145 ksi)

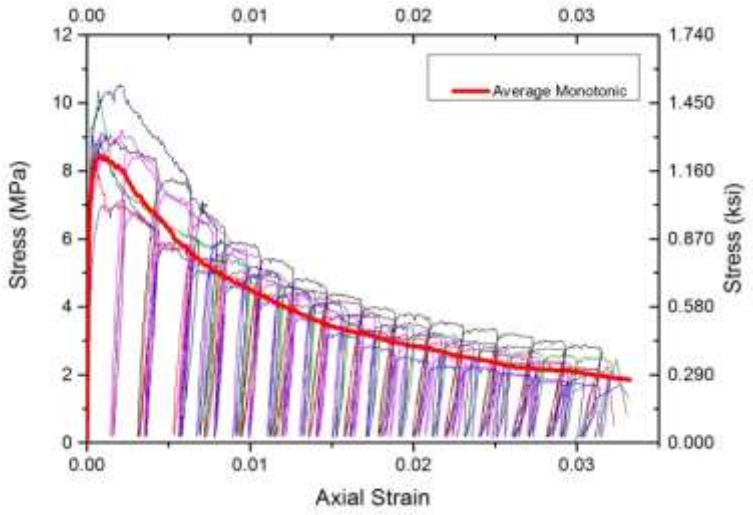

(Note: 1MPa= 0.145 ksi)

Figure 10- Comparison of the average monotonic curve with the cyclic envelope curves

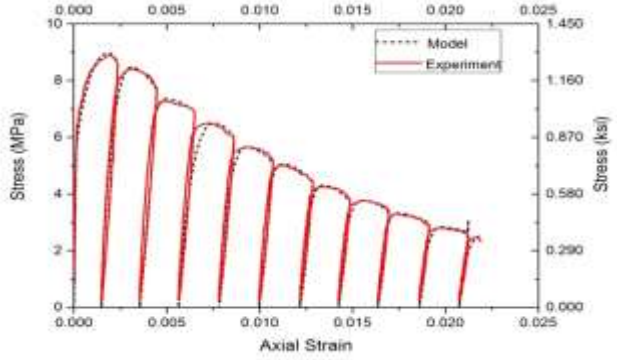

(a)

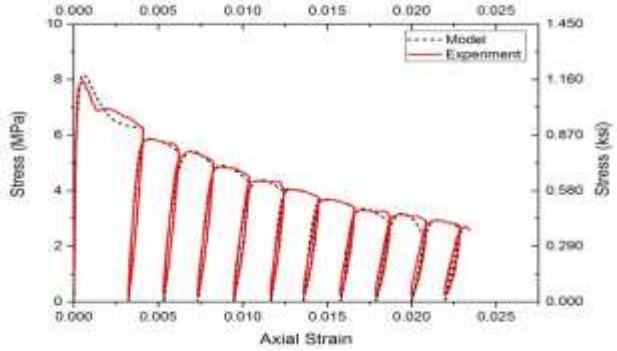

(b)

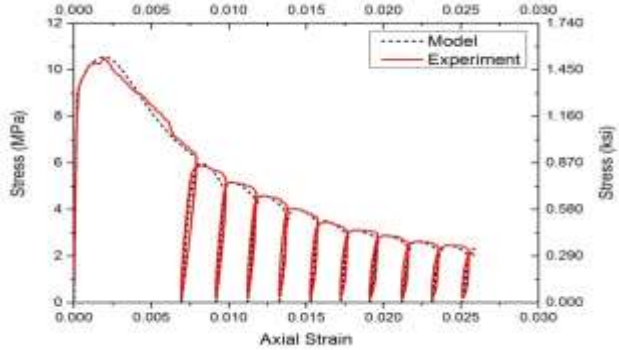

(c)

(Note: 1MPa= 0.145 ksi)

Figure 11- Validation of the proposed model using experimental results for 3 different loading histories and 3% steel fibers

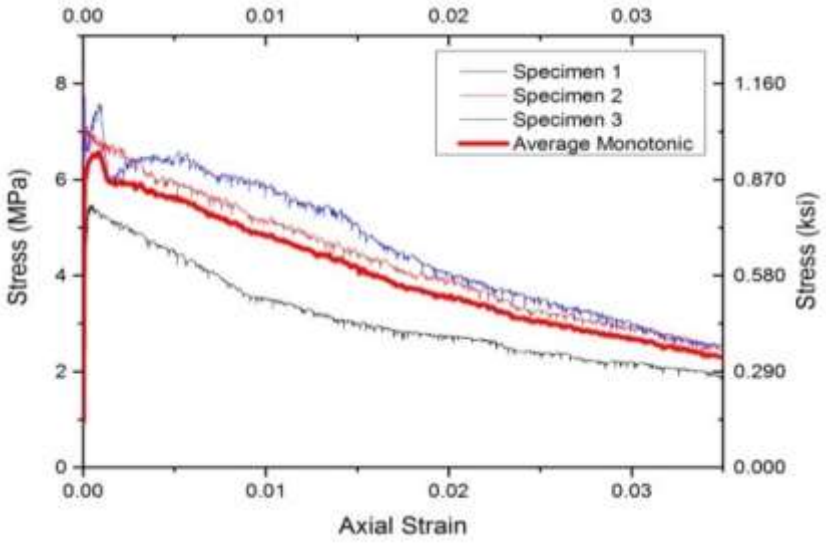

(Note: 1MPa= 0.145 ksi)

Figure 12- Monotonic stress-axial strain curves for specimens with 1% steel fibers

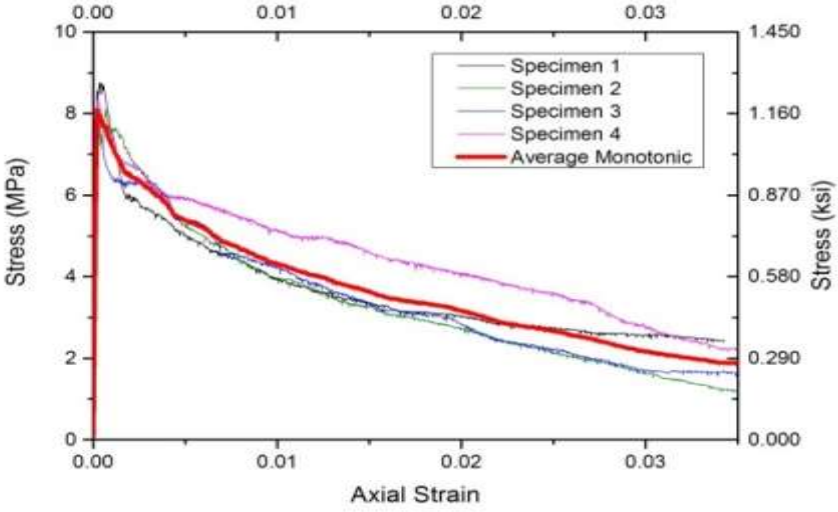

(Note: 1MPa= 0.145 ksi)

Figure 13- Monotonic stress-axial strain curves for specimens with 2% steel fibers

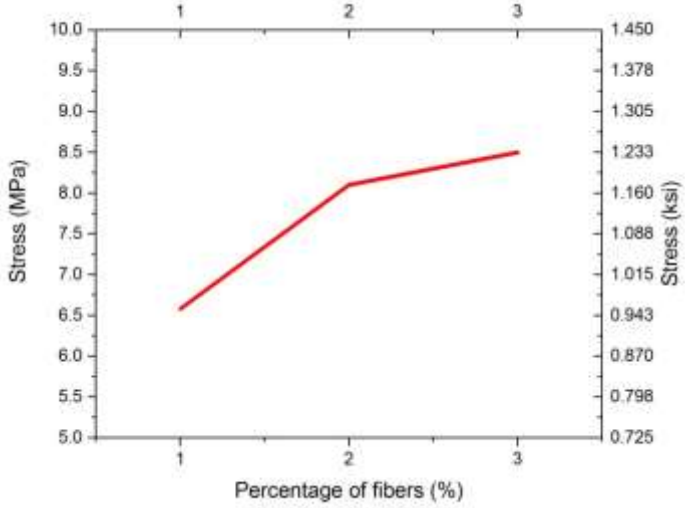

(Note: 1MPa= 0.145 ksi)

Figure 14- Tensile strength for different percentages of steel fibers

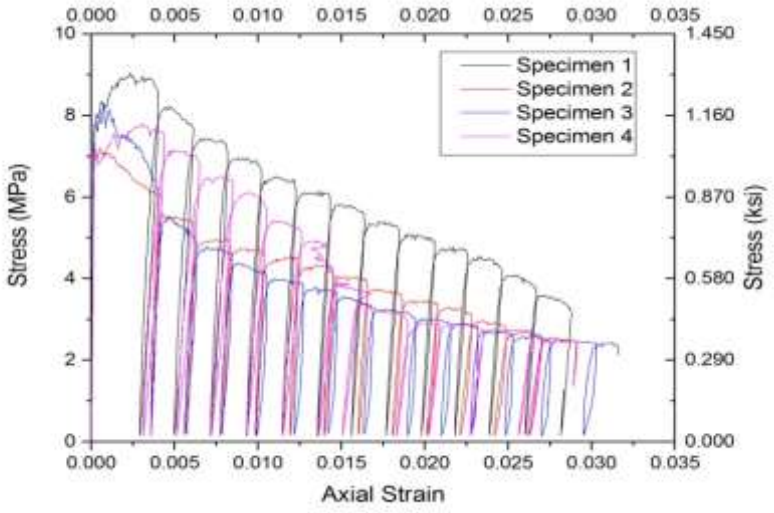

(Note: 1MPa= 0.145 ksi)

Figure 15- Stress-axial strain curves of UHPFRC with 2% steel fibers under cyclic loading

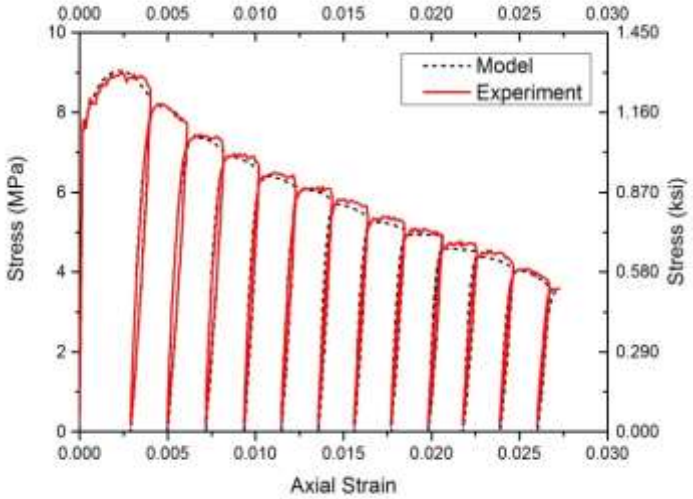

(Note: 1MPa= 0.145 ksi)

Figure 16-Validation of the proposed model for percentage of steel fibers 2%